10-2016

A novel CSI pre-processing scheme for device-free localization indoors

Ju WANG
Northwest University

Lichao ZHANG
Northwest University

Xuan WANG
Northwest University

Jie XIONG
Singapore Management University, jxiong@smu.edu.sg

Xiaojiang CHEN
Northwest University

See next page for additional authors

DOI: https://doi.org/10.1145/2987354.2987361

Author
Ju WANG, Lichao ZHANG, Xuan WANG, Jie XIONG, Xiaojiang CHEN, and Dingyi FANG

Published in S3: Proceedings of the 8th Wireless of the Students, by the Students, and for the Students Workshop: New York, October 3-7, 2016, pp. 6-8. New York: ACM.
http://doi.org/10.1145/2987354.2987361

A Novel CSI Pre-Processing Scheme For Device-Free Localization Indoors

Ju Wang[†], Lichao Zhang[†], Xuan Wang[†], Jie Xiong[♯], Xiaojiang Chen[†], Dingyi Fang[†]
[†]Northwest University; [♯]Singapore Management University;
[†]{wangju,xjchen,dyf}@nwu.edu.cn, [♯]jxiong@smu.edu.sg, [†]{lczhang,wxkate}@stumail.nwu.edu.cn

ABSTRACT

Device-free localization of people and objects indoors not equipped with radios is playing a critical role in many emerging applications. This paper presents a novel channel state information (CSI) pre-processing scheme that enables accurate device-free localization indoors. The basic idea is simple: CSI is sensitive to a target's location and by modelling the CSI measurements of multiple wireless links as a set of power fading based equations, the target location can be determined. However, due to rich multipaths in indoor environment, the received signal strength (RSS) or even the fine-grained CSI can not be easily modelled. We observe that even in a rich multipath environment, not all subcarriers are equally affected by multipath reflections. Our pre-processing scheme tries to identify the subcarriers not affected by multipath. Thus, CSIs on the "clean" subcarriers can be modelled and utilized for accurate localization. Extensive experiments demonstrate the effectiveness of the proposed pre-processing scheme.

Categories and Subject Descriptors

C.2.1 [**Computer-Communication Networks**]: Network Architecture and Design– *Wireless communication*

Keywords

Device-Free Localization; Channel State Information

1. INTRODUCTION

Localization plays a key role in our daily life [6, 7]. Particularly, device-free localization without device attached to the target has attracted a lot of research efforts recently [4]. For instance, in intrusion detection, expecting an uncooperative target to carry a device is not realistic.

Traditional device-free localization systems are mainly based on the coarse-grained RSS signatures [8], resulting in a limited localization accuracy [4]. To improve accuracy, fine-grained CSI has been employed recently [5]. However, raw CSI measurements from commercial off-the-shelf (COTS) devices can not be directly applied to model a target's location because of strong multipath propagations and hardware noises. Thus, previous approaches [5] have difficulties to employ a unified model to accurately quantify the relationship between the CSI measurement and the target's location.

In this paper, we present a novel CSI pre-processing scheme that enables accurate device-free localization in rich multipath indoors. We observe that not all subcarriers are equally affected by multipaths even in a rich multipath environment. Consequently, we introduce a novel CSI pre-processing method to filter out those subcarriers greatly affected by multipath and hardware noise. After this processing, we can quantify the relationship between the pre-processed CSI values and a target's locations with the help of a power fading model. With such a relationship, we can calculate a target's location accurately.

2. BACKGROUND

To passively (device-free) localize a target, we need to understand the effect of a target's location on the CSI measurement. Let λ denote the wavelength of the wireless signal and the wireless link ℓ_{ij} between transmitter i and receiver j has a length of d_{ij}. We refer d_{it} and d_{jt} as the distances from the target to transmitter i and receiver j. According to wireless communication principles [1], the power fading between the two transceivers is mainly related to the *propagation fading*, *diffraction fading* and *target absorption fading*.

Propagation fading: Propagation fading [1] L_{ij} specifies the attenuation due to propagation of a distance d_{ij} between the transmitter i and the receiver j in dBm:

$$L_{ij} \;=\; 10\log[\lambda^2/(16\pi^2 d_{ij}^2)]. \tag{1}$$

Diffraction fading: Diffraction fading D_{ijt} specifies the attenuation due to a target located in the First Fresnel Zone (FFZ) of link ℓ_{ij} [1]. A Fresnel zone is an ellipsoid whose foci are the transmitter and the receiver, as shown in Fig. 4. The radius of the circular cross section of the FFZ is given by $r_1 = \sqrt{(\lambda \cdot d_{it} \cdot d_{jt})/d_{ij}}$. The diffraction fading is significant when a target is located within the FFZ; while the diffraction fading is very small when the target is far away from the FFZ [1]. D_{ijt} is a function of the distances from the target to transmitter i and receiver j, which is given by:

$$D_{ijt} = 20\log\left(\frac{\sqrt{2}}{2}\cdot\left|\int_v^{\infty}\exp(\frac{-\mathbf{J}\cdot\pi z^2}{2})dz\right|\right), \tag{2}$$

where $v = h_t\sqrt{2(d_{it}+d_{jt})/(\lambda \cdot d_{it}\cdot d_{jt})}$ determines the volumes of the diffraction fading and h_t is the target's effective

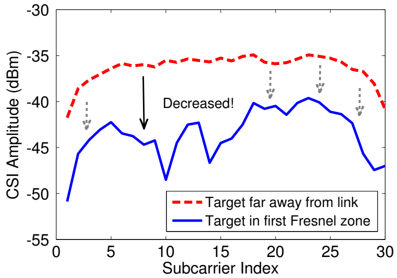

Figure 1: CSI measurements in an outdoor open space with and without a target located in FFZ.

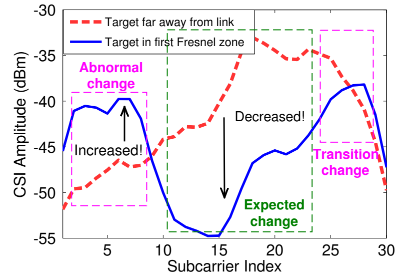

Figure 2: CSI measurements in a typical office room with and without a target located in FFZ.

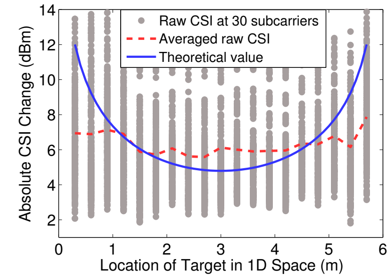

Figure 3: CSI change measurements of the raw data at 30 subcarriers when a target is located at different locations.

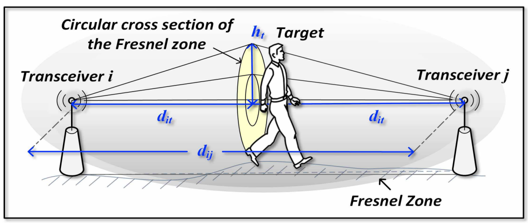

Figure 4: Power fading model.

height. h_t is defined as the distance from the highest point of the target to the wireless link.

Target absorption fading: When a target is located exactly on the LoS path, a link suffers large extra signal attenuation absorbed by the target, which is denoted as A_t ($A_t < 0$) and is dependent on the target.

Putting things together, when a target is located in the monitoring area, the power fading between the transmitter i and the receiver j, i.e., the CSI amplitude measurement R_{ij}, is expressed as below in dBm:

$$R_{ij} = \begin{cases} L_{ij} + D_{ijt} + A_t + \eta, \ LoS, & (3) \\ L_{ij} + D_{ijt} + \eta, \ NLoS \ but \ still \ in \ FFZ, & (4) \\ L_{ij} + \eta, \quad outside \ of \ FFZ, & (5) \end{cases}$$

where η is the measurement noise. "NLoS but still in FFZ" in Eqn. (4) means the target is not on the LoS path but still located in FFZ. We refer Eqn. (3), Eqn. (4) and Eqn. (5) as the power fading model. For simplicity, we use "CSI" to represent "CSI amplitude" in the rest of this paper.

3. PRE-PROCESSING CSI MEASUREMENT

In reality, multipath reflections and hardware noises [5] may also affect the CSI changes. We would like to filter out those subcarriers greatly affected by multipaths and noises, thus only retrieving the CSI changes on the "clean" subcarriers for location estimate.

3.1 CSI Change in Multipath Environment

To understand the CSI changes in rich multipath environment, we conduct experiments in both an outdoor open space and a typical indoor office room. We set the distance between an AP and a laptop equipped with Intel 5300 NIC as 6 m. In each environment, we collect two sets of CSI measurements when a target is located inside and outside the FFZ, and the results are shown in Fig. 1 and Fig. 2.

Fig. 1 illustrates that the CSI amplitudes of all the subcarriers are decreased in the open space environment when a target is located in the FFZ, which is consistent with the diffraction theory [1]. However, in the indoor office environment, the situation is more complicated. Fig. 2 displays that the CSI amplitudes of some subcarriers are increased (e.g., the 5th subcarrier) or remain unchanged (e.g., the 9th subcarrier), which are obviously inconsistent with the diffraction theory. Thus, if we apply the power fading model directly on the raw CSI measurements, these inconsistencies will result in large localization errors. For example, Fig. 3 shows the CSI changes of all subcarriers when we let a target move along the LoS path from the transmitter to the receiver. For evaluation purposes, we also plot the theoretical CSI values in Fig. 3 based on the diffraction theory in Eqn. (2). We can see that the variations of the raw CSI change measurements are quite large, and the averaged values do not match the theoretical curve well.

The CSI changes at all subcarriers in an indoor environment can be categorized into three groups which we term them as *expected change*, *abnormal change* and *transition change* as shown in Fig. 2. The *expected change* has a feature similar to the outdoor open space environment, which is mainly caused by the presence of a target and conforms to the diffraction theory. The *abnormal change* has an opposite effect to the *expected change*, i.e., the CSI amplitude is increased rather than decreased. This *abnormal change* is caused by constructive multipath propagations in the indoor environment. The *transition change* is the "transition zone" between the *expected change* and the *abnormal change*.

3.2 Pre-Processing Scheme for CSI

Our objective is to remove those subcarriers greatly affected by multipath because the CSIs on these subcarriers do not fit the theoretical model. To filter out these *dirty subcarriers* with abnormal CSI changes, our first step stems from the "power increase" observation at some subcarriers. Specifically, when the CSI amplitude of the k-th subcarrier is increased instead of decreased, we know the subcarrier is affected by multipaths and the CSI measurement at this subcarrier should be filtered out. Unfortunately, it is not easy to filter out the *transition part* since it may also exhibit the "power decrease" feature. To address this issue, we adopt a threshold to filter out the subcarriers in the transition part based on whether the power decrease is large enough. Specifically, if a target is not located on the LoS path, the threshold δ_{eff} is defined as the averaged standard deviation over all the K subcarriers:

$$\delta_{eff} = \frac{1}{K} \sum_{k=1}^{K} \frac{f_k}{f_0} \times \delta_k, \tag{6}$$

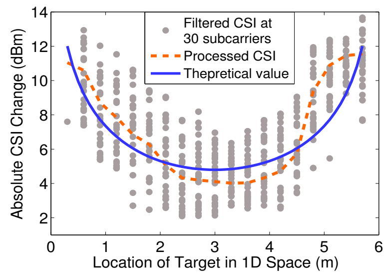

Figure 5: CSI change measurements after pre-processing.

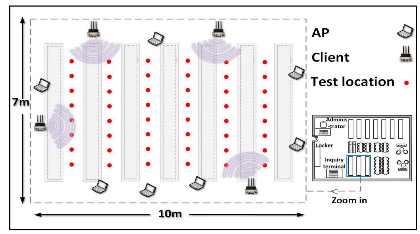

Figure 6: Experimental floorplan of a library (strong NLoS).

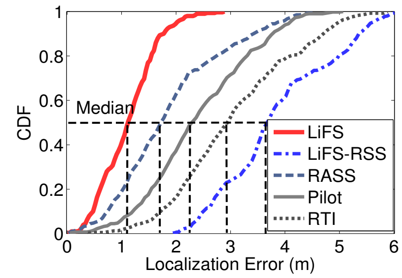

Figure 7: CDF plot of the localization errors in library (strong NLoS).

where f_0 is the central frequency, f_k is the frequency of k-th subcarrier, and δ_k is the standard deviation of the amplitudes of baseline CSI measurements on k-th subcarrier when no target is present. If a target is located on LoS, the threshold δ_{eff} should be added with the absolute signal attenuation $|A_t|$ caused by the target. To identify whether a target is located on the LoS path, the key observations are (i) $|A_t|$ is usually within the range of 4–9 dBm [3] when a human target blocks the LoS path, and (ii) the noise is usually within 1–3 dBm [2]. Thus, a target is more likely located on the LoS path if the averaged CSI change of all subcarriers is larger than 5 dBm. Unless specifically mentioned, we denote δ_{eff} as the threshold for simplicity in the rest of this paper.

Let $\mathbf{F} = \{F_1, F_2, \cdots, F_K\}$ be the CSI measurements when a target is inside the FFZ of a link, and $\mathbf{O} = \{O_1, O_2, \cdots, O_K\}$ be the baseline CSI measurement acquired when we make sure there is no target present in the monitoring area. I is a set of subcarrier indices in which the CSI amplitude decrease is larger than the threshold δ_{eff}, i.e., $I = \{j : F_j - O_j > \delta_{eff}, 1 \leq j \leq K\}$. When a target appears, the *effective CSI* value CSI_{eff} and the *effective CSI change* value ΔCSI_{eff} are calculated as:

$$CSI_{eff} = \frac{1}{|I|} \sum_{j \in I} \frac{f_j}{f_0} \times F_j, \tag{7}$$

$$\Delta CSI_{eff} = \frac{1}{|I|} \sum_{j \in I} \frac{f_j}{f_0} \times (F_j - O_j). \tag{8}$$

We emphasize that the effective CSI value CSI_{eff} is the desirable output of the pre-processing scheme. If a target is located on the LoS path, CSI_{eff} should conform to Eqn. (3), otherwise it should conform to Eqn. (4). The effective CSI change ΔCSI_{eff} should conform to the diffraction fading D in Eqn. (2).

4. VERIFICATION AND EVALUATION

Pre-Processing Scheme Verification: Under the same deployment setup described in Section 3.1, we conduct experiments to validate the effectiveness of our pre-processing scheme. Fig. 5 shows the pre-processed CSI measurements when a target moves along the LoS path between the transmitter and receiver as mentioned in Section 3.1. For each location, we acquire the pre-processed CSI change ΔCSI_{eff} based on Eqn. (8). Compared with the raw CSI measurements which behave quite randomly as shown in Fig. 3, the pre-processed CSI changes are relatively stable and match the model-calculated values well in Fig. 5. it implies our pre-processing scheme effectively retrieves clean subcarriers which conform to diffraction model, and thus ensure a high localization accuracy even in a rich multipath environment.

Localization Performance Evaluation: We conduct experiments in a small part of a library with a size of 7 m × 10 m. The library has shelves, resulting in rich multipaths and a strong NLoS scenario. The experimental floorplan is shown in 6, where the test locations are 0.6 m separated from each other, and a person with a height of 1.72 m acts as the target. We compare the performance of our localization method LiFS with three state-of-the-art schemes, i.e., Pilot [5], RASS [8] and RTI [4]. Fig. 7 shows that LiFS achieves 1.6×, 2.2× and 2.7× higher accuracies than RASS, Pilot and RTI. LiFS with RSS also suffers from large errors since RSS value is an average of all the subcarriers including those “dirty subcarriers”.

5. REFERENCES

[1] A. F. Molisch. *Wireless communications*. John Wiley & Sons.

[2] J. Wang, X. Chen, D. Fang, C. Q. Wu, Z. Yang, and T. Xing. Transferring compressive-sensing-based device-free localization across target diversity. *IEEE Trans. on Industrial Electronics*, 62(4):2397–2409, 2015.

[3] J. Wang, D. Fang, Z. Yang, H. Jiang, X. Chen, T. Xing, and L. Cai. E-hipa: An energy-efficient framework for high-precision multi-target-adaptive device-free localization. *IEEE Trans. on Mobile Computing*, 12(5):1–12, 2016.

[4] J. Wilson and N. Patwari. See-through walls: Motion tracking using variance-based radio tomography networks. *IEEE Trans. on Mobile Computing*, 10(5):612–621, 2011.

[5] J. Xiao, K. Wu, Y. Yi, L. Wang, and L. M. Ni. Pilot: Passive device-free indoor localization using channel state information. In *Proc. IEEE ICDCS*, pages 236–245, 2013.

[6] J. Xiong and K. Jamieson. Arraytrack: a fine-grained indoor location system. In *Proc. USENIX NSDI*, pages 71–84, 2013.

[7] J. Xiong, K. Sundaresan, and K. Jamieson. Tonetrack: Leveraging frequency-agile radios for time-based indoor wireless localization. In *Proc. ACM MobiCom*, pages 537–549, 2015.

[8] D. Zhang, Y. Liu, X. Guo, and L. M. Ni. Rass: A real-time, accurate, and scalable system for tracking transceiver-free objects. *IEEE Trans. on Parallel and Distributed Systems*, 24(5):996–1008, 2013.